Sensors and Actuators B 156 (2011) 593–598

Contents lists available at ScienceDirect

Sensors and Actuators B: Chemical

journal homepage: www.elsevier.com/locate/snb

High-speed optical humidity sensors based on chiral sculptured thin films

Yan Jun Liu, Jinjie Shi, Fan Zhang, Huinan Liang, Jian Xu, Akhlesh Lakhtakia, Stephen J. Fonash, Tony Jun Huang*

Department of Engineering Science and Mechanics, Pennsylvania State University, University Park, PA 16802, USA

ARTICLE INFO

Article history:
Received 24 June 2010
Received in revised form 14 January 2011
Accepted 3 February 2011
Available online 12 February 2011

Keywords:
Circular Bragg regime
Humidity sensor
High speed
Sculptured thin films
Nanowire

ABSTRACT

A high-speed humidity sensor based on a nanostructured chiral sculptured thin film (CSTF) was fabricated and tested. The sensing principle is based on the shift of the central wavelength of the circular Bragg regime of the CSTF caused by adsorption and desorption of water vapor in the void regions of the CSTF. Spectral changes due to varying relative-humidity (RH) levels in the ambient environment were measured by a spectrometer. The CSTF sensor exhibited excellent reversibility and reproducibility from 40% to 100% RH. Moreover, the adsorption time of the sensor was measured to be as low as ~140 ms, making it promising for many high-speed humidity-sensing applications.

1. Introduction

Humidity sensors have many different applications ranging from nuclear power reactors to residential air conditioners [1–4]. In recent decades, various sensing modalities have been developed, typically exploiting changes in resistance, capacitance, or refractive index (RI) to characterize changes in relative humidity (RH) [5–8]. The most widely used humidity-sensing materials include porous ceramics (*e.g.*, Al_2O_3 and TiO_2) [9–14], nanostructured metal oxides [15–17], polymers (*e.g.*, polyimide and phthalocyanine) [18–20], and polyelectrolytes (*e.g.*, sulfonated polysulfone and polyvinyl acetate) [21,22].

The criteria for a desirable humidity sensor include high sensitivity, long-term durability, fast response, low cost, and operation over a wide range of humidity and temperature. A particularly important parameter of humidity sensors is their response speed. A response time on the order of several seconds is considered high-speed for humidity sensors today [23,24]. However, humidity sensors with sub-second response times will be crucial for numerous applications including control of industrial processes, monitoring atmospheric RH, managing patients undergoing anesthesia, and pulmonary-function diagnostics [25,26]. Sub-second humidity sensors using inorganic materials have been demonstrated based on porous nanostructures with different materials and architectures [27–34]. Humidity sensors using organic materials have also been developed using photoresist and polyimide [27,35]. Humidity-sensing devices [36,37] using nanoporous polymer structures have been made by holographic photopolymerization [38,39]. Table 1 summarizes the typical response time of the reported high-speed humidity sensors. Among the aforementioned humidity sensors, metal oxide based sensors are promising in terms of their response speed, stability, and repeatability. Most of these sensors are capacitive, involving electrical measurements. Relatively few optical sensors have been demonstrated, and they are generally based on a narrow bandpass filter using TiO_2 nanostructures [40–42].

In this paper, we report the fabrication and characterization of an optical humidity sensor based on a chiral sculptured thin film (CSTF). The CSTFs consist of arrays of helical nanowires that are parallel and nominally identical to each other, providing the CSTF with a distinguished axis of chirality that is aligned normal to the substrate on which the CSTF is deposited [43]. This helical morphology gives rise to a resonance for either left- or right-circularly polarized (LCP or RCP) light, with the resonance regime being called the circular Bragg regime [43–45]. Most importantly, when the wave vector of the incident CP light is parallel to the axis of chirality and the CSTF is sufficiently thick, CP light of the same handedness as the CSTF is highly reflected, but CP light of the other handedness is only slightly reflected in the circular Bragg regime. A CSTF is thus a circular polarization filter [45]; this characteristic has also been exploited to realize CP light emission from light-emitting devices made of CSTFs [46,47]. The circular polarization-sensitive properties of a CSTF depend on

* Corresponding author. Tel.: +1 814 863 4209; fax: +1 814 865 9974.
E-mail address: junhuang@psu.edu (T.J. Huang).

0925-4005/$ – see front matter © 2011 Elsevier B.V. All rights reserved.
doi:10.1016/j.snb.2011.02.003

Table 1
Reported adsorption and desorption times of various humidity sensors.

Material	Adsorption time	Desorption time	Reference no.
Porous silicon oxide	35 ms	25 ms	[27]
Nanoporous silicon thin film	200 ms	N.A.	[28]
Rhodium electroplated sensor	30–50 ms	30–50 ms	[29]
Nanostructured metal oxide	<220 ms	>400 ms	[30–33]
Polyimide columnar film	1 s	N.A.	[35]
Helical photoresist structure	75 ms	175 ms	[27]
Porous polymeric grating	137 ms	9 s	[36]
Porous polymeric photonic crystal	1.5 s	20–30 s	[37]

the material chosen to fabricate it, the deposition pressure and temperature, and most significantly, the direction of the adatom flux with respect to the substrate during deposition. Generally, smaller angles between the adatom-flux direction and the substrate correspond to more porous CSTFs [43]. To our knowledge, the circular Bragg regime has been experimentally validated for humidity sensing only by Lakhtakia et al. [44], that too only qualitatively.

The central wavelength and the full-width-at-half-maximum (FWHM) bandwidth of the circular Bragg regime are dependent on the permittivity mismatch between the helical nanowires and the void regions of the CSTF, in addition to its porosity [48,49]. Examination of scanning electron micrographs indicates that the void regions exist on two length scales: between the helical nanowires (submicron scale) and inside the nanowires (nanoscale) [43]. Upon exposure to varying RH, the water vapor diffuses in/out of the void regions, inducing changes in the overall dielectric properties of the CSTF, as well as the parameters of the circular Bragg regime. Theory predicts that the spectral shift of the circular Bragg regime can be used to quantitatively sense the RH change of the environment [48,49]. As we will demonstrate in Section 3, this inorganic-material-based humidity sensor offers high-speed sensing, long-term stability, and desirable reproducibility. Additionally, as electron-beam evaporation is a workhorse technique commonly used by manufacturers [43,50], this optical humidity sensor will also be inexpensive.

2. Description of experiments

CSTFs were deposited through an electron-beam evaporation system configured for the serial bideposition (SBD) technique [45,51], in which the substrate was tilted at an angle of 15° measured between the direction of the impinging vapor flux and the substrate plane; this angle is denoted by χ_v in Fig. 1. By periodically rotating the substrate 180° about the substrate normal (the z-axis in Fig. 1) during the deposition process, a CSTF with desired helical morphology can be obtained. The pitch of the helical nanowires in the CSTF is defined as the width of one complete turn along the axis. The void region between the helical nanowires and the volume fraction of the deposited material can also be experimentally controlled with this process.

The CSTFs were deposited onto flat 1 in. × 1 in. glass substrates (Corning 7059). The distance between the evaporation source and the center of the substrate was 10 in., and the deposition rate was controlled at 2.5 Å/s, which was monitored by a resonating quartz crystal sensor at normal incidence located near the substrate. A well-controlled deposition rate resulted in a uniform pitch. The vacuum base pressures were below 4×10^{-6} Torr. Titanium dioxide (TiO_2) was chosen as the material for deposition, because of its high bulk refractive index ($n_{TiO_2} = 2.6$) and excellent transparency at visible wavelengths. In addition, TiO_2 demonstrates the photocatalytic self-cleaning phenomenon: ultraviolet illumination of TiO_2 generates electron-hole pairs that react with organic contaminants on the surface to produce several compounds including CO_2 and H_2O [34,52], which desorb from the surface. This self-cleaning effect provides a solution to reduce the impact of sensor aging. Finally, the optical properties of TiO_2 do not change significantly over common environmental temperature ranges.

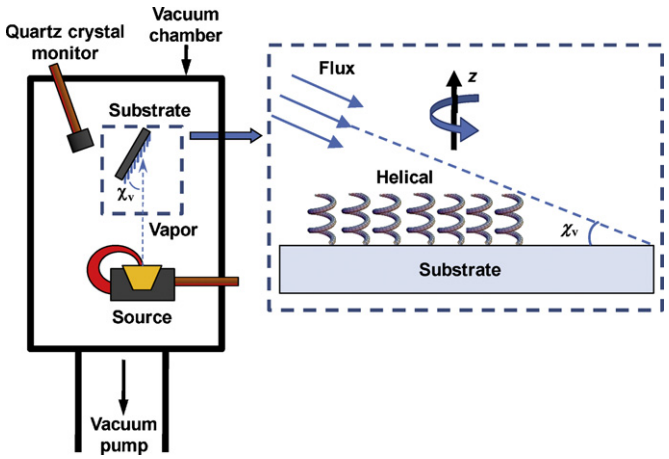

Fig. 1. Schematic of the oblique angle deposition process.

Our setup for the rapid optical sensing of humidity is illustrated in Fig. 2. A structurally right-handed CSTF was attached to a Teflon substrate. Light from a halogen lamp was made either LCP or RCP through a combination of a linear polarizer and a quarter-wave plate, and was then used to illuminate the CSTF normally. The total transmittance through the CSTF was measured over the 500–900 nm wavelength range with a spectrometer (Ocean Optics Co., HR4000). A humidity chamber (ESPEC North America Inc., SH-241) integrated with a water tank and a fan system was used to control the operating temperature and the RH. The RH inside the humidity chamber could be programmed and adjusted to any value between 40% and 95%.

However, because the humidity chamber required almost 15 min to adjust the RH, we were forced to use a separate method to characterize the sensor's response time. This was done using a small, transparent chamber (4 cm × 4 cm × 4 cm), where the RH can be made to quickly oscillate between 20% and 100%. RCP light from an external He–Ne laser diode ($\lambda = 633$ nm) was guided normally through the structurally right-handed CSTF, where the transmitted intensity was collected by a photodetector. Step-like intensity changes (corresponding to the transmittance changes in the circular Bragg regime of the CSTF induced by the RH oscillations within the chamber) were captured through the photodetector. The response time was then extracted from the recorded data.

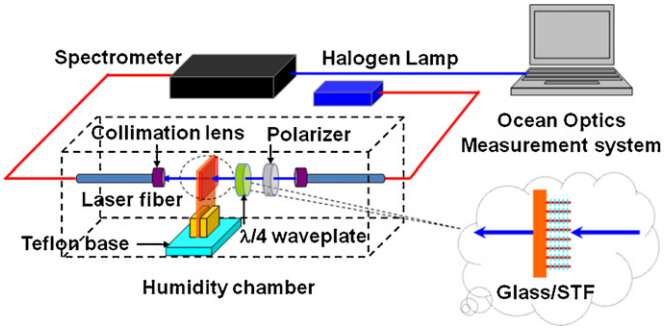

Fig. 2. Schematic of the humidity-sensing measurement setup.

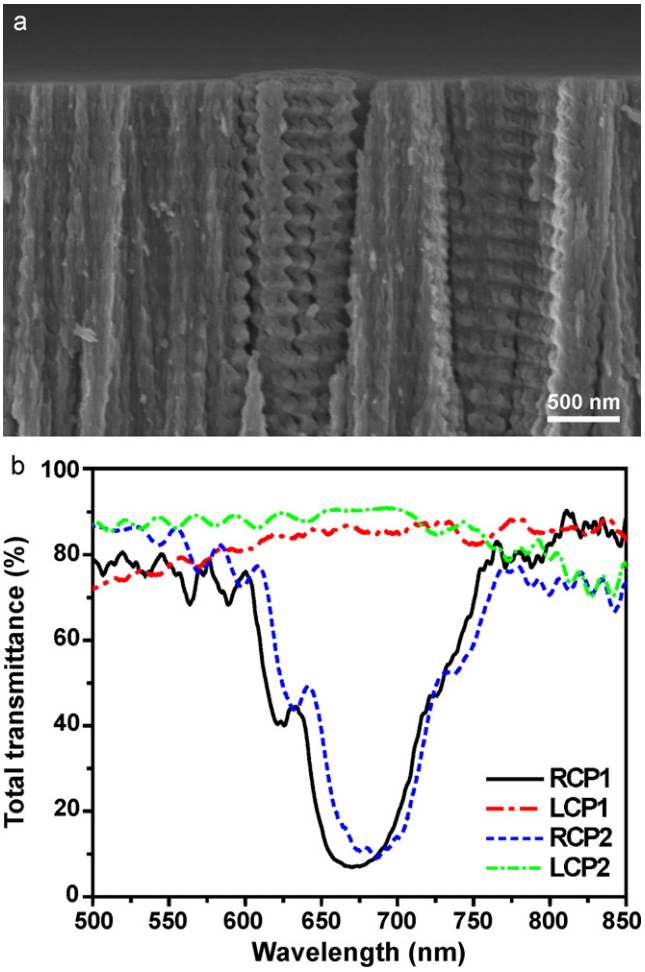

Fig. 3. (a) Cross-sectional scanning electron micrograph of a structurally right-handed CSTF and (b) its total-transmittance spectra for normally incident circularly polarized light for the sample measured as-deposited (RCP1/LCP1) and after one year (RCP2 and LCP2).

3. Results and discussion

As the helical nanowires of the chosen CSTF – whose scanning electron micrograph is shown in Fig. 3(a) – had a pitch of 320 nm, and the CSTF had ~7.5 structural periods in the thickness direction, it was ~2.42 μm thick. Fig. 3(b) shows the total-transmittance spectra of the CSTF measured for normally incident LCP and RCP light at room temperature. A well-defined circular Bragg regime is presented as a deep trough in the total-transmittance spectrum for incident RCP light, with a minimum 10% of light transmitted; whereas there is uniformly high transmission of incident LCP light over the same spectral regime. The central wavelength of the circular Bragg regime is ~670 nm and the FWHM bandwidth is ~80 nm.

The ratio ν of the central wavelength to the pitch is a function of the three principal refractive indexes of the CSTF and of the angle of rise of the helical nanowires [43]. The ratio, whose value $\nu = 670/320 = 2.094$ for the chosen CSTF, can be considered as an equivalent refractive index. While a detailed homogenization model of CSTFs based on the Bruggeman approach for optically biaxial materials (such as CSTFs) is under development [48,49,53,54], the very simple Arago-Biot approach [55] predicts the value of the equivalent refractive index as $n_{TiO_2} f_{TiO_2} + (1 - f_{TiO_2}) = 2.12$, with the volume fraction of titanium oxide estimated as $f_{TiO_2} = 0.7$. Based on an examination of the scanning electron micrographs of the CSTF, this volume fraction of the solid material in the CSTF appears reasonable. The small difference between the measured and the predicted values of ν is due to (i) the deposited material being TiO_x instead of TiO_2 [56], (ii) electromagnetic absorption indicating dissipative properties [43,54], and (iii) the adsorption of water vapor within the void regions of the CSTF in ambient conditions [57].

Fig. 4 shows that as RH was increased/decreased, the trough in the total-transmittance spectrum for RCP incidence redshifted/blueshifted and the total transmittance in the trough increased/decreased. Such behavior is in good agreement with theoretical predictions based on homogenization models for CSTFs [44,48,49]. Any CSTF can be considered as a two-phase composite material with locally biaxial dielectric properties [43,55]. When the water vapor diffuses into the void regions, the dielectric properties of the CSTF are modified in two ways. First, the three principal refractive indexes of the CSTF – and therefore ν increase to cause the redshift of the circular Bragg regime. Second, the local birefringence of the CSTF decreases, which causes the bandwidth of the circular Bragg regime to decrease; for a fixed pitch and a fixed thickness, the total transmittance in the trough would then increase [43]. Both features are evident in Fig. 4(a), and are more pronounced at higher humidity because more water molecules are adsorbed in the void regions. As the water molecules desorbed with a decrease in the

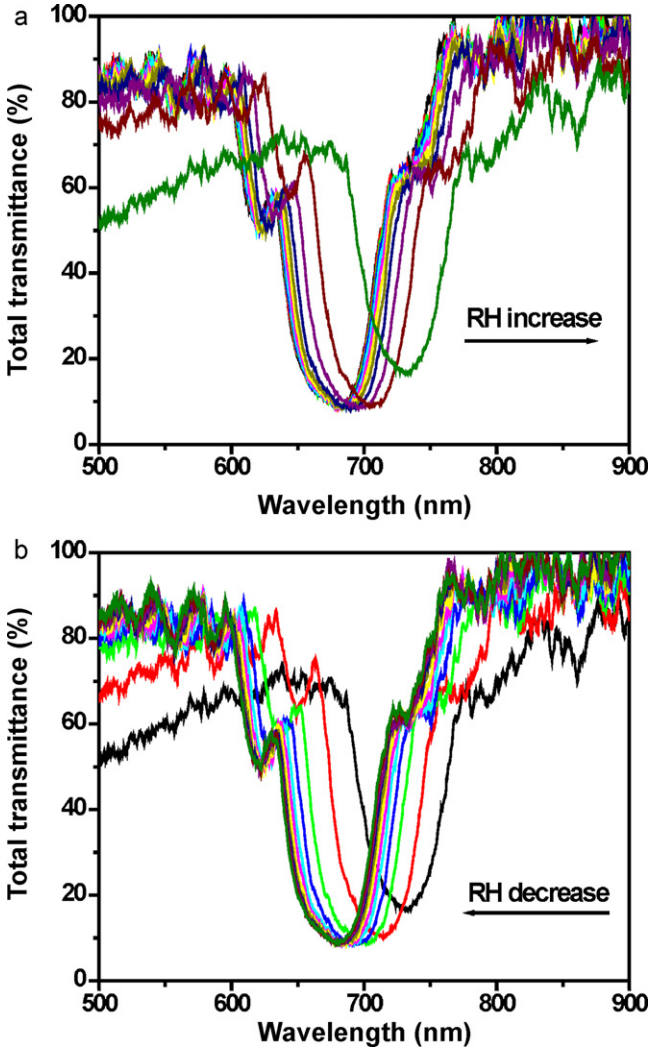

Fig. 4. The total-transmittance spectra of a CSTF with (a) increasing RH and (b) decreasing RH. The incident light is RCP to match the structural right-handedness of the CSTF.

RH, the total-transmittance spectrum returned to the initial state, as displayed in Fig. 4(b).

The measured central wavelength as a function of RH is presented in Fig. 5, for both increasing and decreasing RH. Minor hysteresis is evident when RH is greater than 65%, while the hysteresis is negligible below this level. This minor hysteresis resulted from desorption, which was relatively fast because titanium-oxide films are generally hydrophobic [58]. From Fig. 5, the detection sensitivity was measured to be ~0.93 nm per RH unit, which is much larger than the reported 0.34 nm per RH unit in the previous work [40].

The stability and repeatability of the humidity sensor over a large RH range was evaluated in a multi-cycle experiment, wherein saturated water vapor (100% RH) was periodically introduced into and removed from the smaller humidity chamber (20% RH background). Fig. 6(a) shows that as the RH periodically oscillated between 20% and 100%, the total transmittance measured at 715 nm wavelength switched between 10% and 50%. The response of the device is highly stable – only small variations (<4%) were observed among more than 100 experimental cycles. Fig. 6(a) shows only the first ten cycles. We also measured the spectra for the CSTF one year after the deposition and found that the circular Bragg regime of the CSTF only slightly red-shifted, as shown in Fig. 3(b), indicating excellent reproducibility and long-term stability of the CSTF-based optical humidity sensor.

Fig. 6(b) indicates that the response time of the adsorption process – as the RH was increased from 20% to 100% – was about 140 ms, while the time for the desorption process was about 1.2 s. Although these values can be compared to their published counterparts summarized in Table 1, we must carefully assure that the measurement protocols are the same before that comparison can be made. The difference in the response times for the adsorption process and the desorption process in our experiments arose for two reasons. First, water molecules usually diffuse slower from the void regions of a thin film to the ambient environment than they do along the opposite route [36]. Second, a fan was employed to introduce a water-vapor-saturated nitrogen stream into the humidity chamber during adsorption, while water vapor was allowed to naturally diffuse during the desorption process from the humidity chamber to the ambient environment. Unassisted diffusion is a much slower process than assisted diffusion.

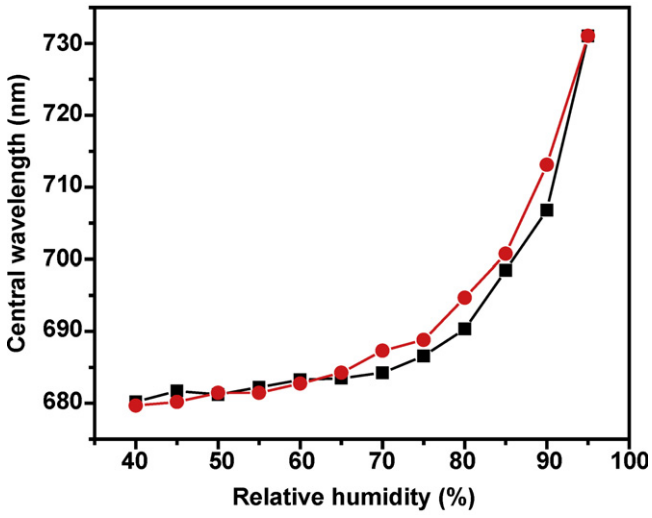

Fig. 5. Central wavelength of the circular Bragg regime with increasing RH (squares joined by a black curve) and decreasing RH (circles joined by a red curve). (For interpretation of the references to color in this figure legend, the reader is referred to the web version of this article.)

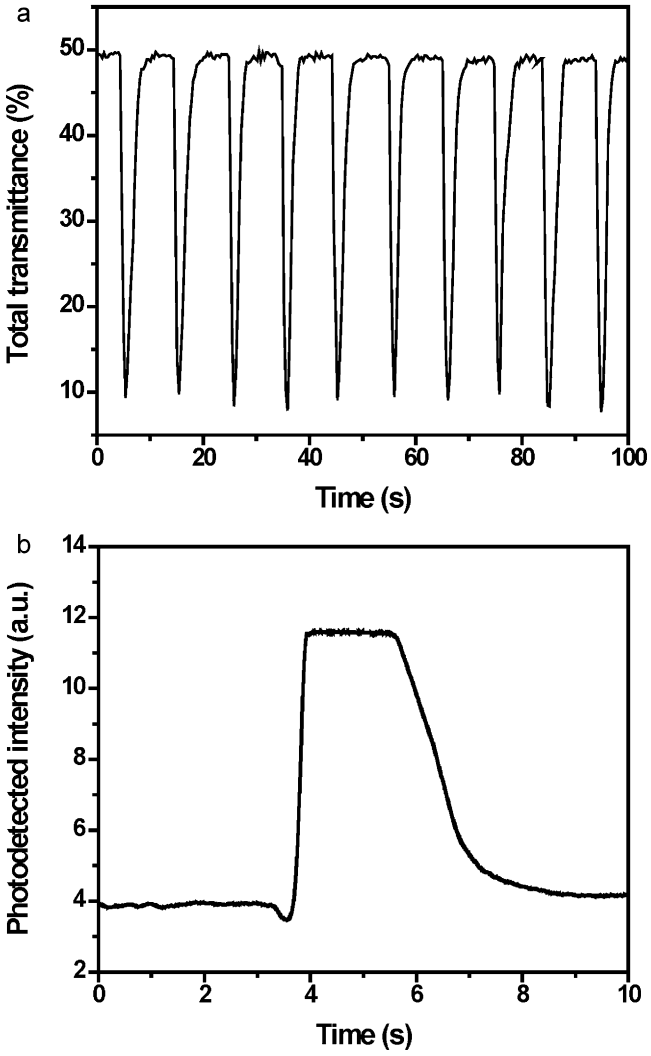

Fig. 6. (a) Time-dependent total transmittance at 715 nm wavelength as the RH oscillates between 20% and 100% for ten cycles. (b) Photodetected intensity recorded as the RH increases from 20% to 100% in the 20th cycle. The ambient temperature was fixed at 40 °C, and only RCP light was incident on the CSTF.

The response time and sensitivity of the sensor are also dependent upon the porosity of the CSTF. In general, void regions with linear dimensions larger than 100 nm are required for a rapid response [13,59]. Steele et al. systematically investigated the response time of capacitative humidity sensors based on columnar thin films of TiO_2 [33]. Extrapolating from that study, we conclude that by optimizing the porosity, thickness, and period of a CSTF, the performance of our optical humidity sensors could be improved to fulfill requirements for response time and/or detection sensitivity. Better performance may also be possible by creating a central 90°-twist defect in the CSTF during deposition, which would then lead to a narrowband feature called a spectral reflection hole [44,60].

4. Concluding remarks

We have experimentally demonstrated the operation of a high-speed optical humidity sensor whose essential element is a chiral sculptured thin film, the operating principle being the shift of the central wavelength of the circular Bragg regime of the CSTF with changes in the relative humidity of the ambient environment. The fabricated sensor exhibited excellent sensitivity, reversibility, and reproducibility over a large range of RH. Furthermore, because the CSTF was made of a material that is chemically inert to water vapor,

the sensor promises excellent repeatability. The sensor displayed a fast response (~140 ms), making it desirable for various high-speed applications. With these advantages, we expect that the CSTF-based optical humidity sensor presented here can be used for a variety of applications such as food science and health care.

Acknowledgements

This research was supported by NIH Director's New Innovator Award (1DP2OD007209-01), Air Force Office of Scientific Research (AFOSR), the Air Force Office of Scientific Research, the National Science Foundation, the Penn State Center for Nanoscale Science (MRSEC), and the Charles Godfrey Binder Endowment at Penn State. Components of this work were conducted at the Penn State node of the NSF-funded National Nanotechnology Infrastructure Network.

References

[1] N. Yamazoe, Shimizu Y, Humidity sensors: principles and applications, Sens. Actuators 10 (1986) 379–398.
[2] R. Fenner, Zdankiewicz E, Micro-machined water vapor sensors: a review of sensing technologies, IEEE Sens. 14 (2001) 309–317.
[3] J.-R. Huang, M.-Q. Li, Z.-Y. Huang, J.-H. Liu, A novel conductive humidity sensor based on field ionization from carbon nanotubes, Sens. Actuators A: Phys. 133 (2007) 467–471.
[4] C.-Y. Lee, G.-B. Lee, Humidity sensors: a review, Sens. Lett. 3 (2005) 1–15.
[5] B. Yang, B. Aksak, Q. Lin, M. Sitti, Compliant and low-cost humidity sensors using nano-porous polymer membranes, Sens. Actuators B: Chem. 114 (2006) 254–262.
[6] S.-J. Kim, J.-Y. Park, S.-H. Lee, S.-H. Yi, Humidity sensors using porous silicon layer with mesa structure, J. Phys. D: Appl. Phys. 33 (2000) 1781–1784.
[7] C.-Y. Lee, G.-B. Lee, Micromachine-based humidity sensors with integrated temperature sensors for signal drift compensation, J. Micromech. Microeng. 13 (2003) 620–625.
[8] S. Muto, O. Suzuki, T. Amano, M Morisawa, A plastic optical fibre sensor for real-time humidity monitoring, Meas. Sci. Technol. 14 (2003) 746–750.
[9] E. Traversa, Ceramic sensors for humidity detection: the state-of-the-art and future developments, Sens. Actuators B: Chem. 23 (1995) 135–156.
[10] Y. Shimizu, H. Arai, T. Seiyama, Theoretical studies on the impedance-humidity characteristics of ceramic humidity sensors, Sens. Actuators 7 (1985) 11–22.
[11] U. Kang, K.D. Wise, A high-speed capacitive humidity sensor with on-chip thermal reset, IEEE Trans. Electron Devices 47 (2000) 702–710.
[12] E.J. Connolly, H.T.M. Pham, J. Groeneweg, P.M. Sarro, P.J French, Relative humidity sensors using porous SiC membranes and Al electrodes, Sens. Actuators B: Chem. 100 (2004) 216–220.
[13] T. Seiyama, N. Yamazoe, H. Arai, Ceramic humidity sensors, Sens. Actuators 4 (1983) 85–96.
[14] L.M. Zambov, C. Popov, M.F. Plass, A. Bock, M. Jelinek, J. Lancok, K. Masseli, W. Kulisch, Capacitance humidity sensor with carbon nitride detecting element, Appl. Phys. A 70 (2000) 603–606.
[15] Z. Li, H. Zhang, W. Zheng, W. Wang, H. Huang, C. Wang, A.G. MacDiarmid, Y. Wei, Highly sensitive and stable humidity nanosensors based on LiCl doped TiO_2 electrospun nanofibers, J. Am. Chem. Soc. 130 (2008) 5036–5037.
[16] Q. Qi, T. Zhang, S. Wang, X. Zheng, Humidity sensing properties of KCl-doped ZnO nanofibers with super-rapid response and recovery, Sens. Actuators B: Chem. 137 (2009) 649–655.
[17] X. Song, Q. Qi, T. Zhang, C. Wang, A humidity sensor based on KCl-doped SnO_2 nanofibers, Sens. Actuators B: Chem. 138 (2009) 368–373.
[18] Z. Yao, M. Yang, A fast response resistance-type humidity sensor based on organic silicon containing cross-linked copolymer, Sens. Actuators B: Chem. 117 (2006) 93–98.
[19] A. Tsigara, G. Mountrichas, K. Gatsouli, A. Nichelatti, S. Pispas, N. Madamopoulos, N.A. Vainos, H.L. Du, F. Roubani-Kalantzopoulou, Hybrid polymer/cobalt chloride humidity sensors based on optical diffraction, Sens. Actuators B: Chem. 120 (2007) 481–486.
[20] B. Yang, B. Aksak, Q. Lin, M. Sitti, Compliant and low-cost humidity nanosensors using nanoporous polymer membranes, Sens. Actuators B: Chem. 114 (2006) 254–262.
[21] C.P.L. Rubinger, C.R. Martins, M.A. De Paoli, R.M. Rubinger, Sulfonated polystyrene polymer humidity sensor: synthesis and characterization, Sens. Actuators B: Chem. 123 (2007) 42–49.
[22] B. Adhikari, S. Majumdar, Polymers in sensor applications, Prog. Polym. Sci. 29 (2004) 699–766.
[23] E.J. Connolly, G.M. O'Halloran, H.T.M. Pham, P.M. Sarro, P.J. French, Comparision of porous polysilicon and porous silicon carbide as materials for humidity sensing applications, Sens. Actuators A: Phys. 99 (2002) 25–30.
[24] Z.M. Rittersma, A. Splinter, A. Bödecker, W. Benecke, A novel surface-machined capacitive porous silicon humidity sensor, Sens. Actuators B: Chem. 68 (2000) 210–217.
[25] C. Laville, C. Pellet, Comparison of three humidity sensors for a pulmonary function diagnosis microsystem, IEEE Sens. J. 2 (2002) 96–101.
[26] T. Tatara, K. Tsuzaki, An apnea monitor using a rapid-response hygrometer, J. Clin. Monit. 13 (1997) 5–9.
[27] K.D. Harris, A. Huizinga, M.J. Brett, High-speed porous thin film humidity sensors, Electrochem. Solid State Lett. 5 (2002) H27–H29.
[28] A.K. Kalkan, H.D. Li, C.J. O'Brien, S.J. Fonash, A rapid-response, high-sensitivity nanophase humidity sensor for respiratory monitoring, IEEE Electron Devices Lett. 25 (2004) 526–528.
[29] P. Kuban, J.M. Berg, P.K. Dasgupta, Durable microfabricated high-speed humidity sensors, Anal. Chem. 76 (2004) 2561–2567.
[30] J.J. Steele, G.A. Fitzpatrick, M.J. Brett, Capacitive humidity sensors with high sensitivity and subsecond response times, IEEE Sens. J. 7 (2007) 955–956.
[31] J.J. Steele, M.T. Taschuk, M.J. Brett, Nanostructured metal oxide thin films for humidity sensors, IEEE Sens. J. 8 (2008) 1422–1429.
[32] M.R. Kupsta, M.T. Taschuk, M.J. Brett, J.C. Sit, Reactive ion etching of columnar nanostructured TiO_2 thin films for modified relative humidity sensor response time, IEEE Sens. J. 9 (2009) 1979–1986.
[33] J.J. Steele, M.T. Taschuk, M.J. Brett, Response time of nanostructured relative humidity sensors, Sens. Actuators B: Chem. 140 (2009) 610–615.
[34] M.T. Taschuk, J.J. Steele, A.C. Van Popta, M.J. Brett, Photocatalytic regeneration of interdigitated capacitor relative humidity sensors fabricated by glancing angle deposition, Sens. Actuators B: Chem. 134 (2008) 666–671.
[35] U. Kang, K.D. Wise, A high-speed capacitive humidity sensor with on-chip thermal reset, IEEE Trans. Electron Devices Lett. 47 (2000) 702–710.
[36] J. Shi, V.K.S. Hsiao, T.J. Huang, Nanoporous polymeric transmission gratings for high-speed humidity sensing, Nanotechnology 18 (2007) 465501.
[37] J. Shi, V.K.S. Hsiao, T.R. Walker, T.J. Huang, Humidity sensing based on nonporous polymeric photonic crystals, Sens. Actuators B: Chem. 129 (2008) 391–396.
[38] T.J. Bunning, L.V. Natarajan, V.P. Tondiglia, R.L. Sutherland, Holographic polymer-dispersed liquid crystals (H-PDLCS), Annu. Rev. Mater. Sci. 30 (2000) 83–115.
[39] Y.J. Liu, B. Zhang, Y. Jia, K.S. Xu, Improvement of the diffraction properties in holographic polymer dispersed liquid crystal Bragg gratings, Opt. Commun. 218 (2003) 27–32.
[40] J.J. Steele, A.C. van Popta, M.M. Hawkeye, J.C. Sit, M.J. Brett, Nanostructured gradient index optical filter for high-speed humidity sensing, Sens. Actuators B: Chem. 120 (2006) 213–219.
[41] A.C. Van Popta, J.J. Steele, S. Tsoi, J.G.C. Veinot, M.J. Brett, J.C. Sit, Porous nanostructured optical filters rendered insensitive to humidity by vapour-phase functionalization, Adv. Funct. Mater. 16 (2006) 1331–1336.
[42] D.H. Chang, Y.J. Park, C.K. Hwangbo, Optical humidity sensor using a narrow band-pass filter prepared by glancing angle deposition, J. Korean Phys. Soc. 53 (2008) 2700–2704.
[43] A. Lakhtakia, R. Messier, Sculptured Thin Films: Nanoengineered Morphology and Optics Bellingham, SPIE Press, WA, USA, 2005.
[44] A. Lakhtakia, M.W. McCall, J.A. Sherwin, Q.H. Wu, I.J. Hodgkinson, Sculptured-thin-film spectral holes for optical sensing of fluids, Opt. Commun. 194 (2001) 33–46.
[45] Q. Wu, I.J. Hodgkinson, A. Lakhtakia, Circular polarization filters made of chiral sculptured thin films: experimental and simulation results, Opt. Eng. 39 (2000) 1863–1868.
[46] F. Zhang, J. Xu, A. Lakhtakia, S.M. Pursel, M.W. Horn, A. Wang, Circularly polarized emission from colloidal nanocrystal quantum dots confined in microcavities formed by chiral mirrors, Appl. Phys. Lett. 91 (2007) 023102.
[47] F. Zhang, J. Xu, A. Lakhtakia, T. Zhu, S.M. Pursel, M.W. Horn, Circular polarization emission from an external cavity diode laser, Appl. Phys. Lett. 92 (2008) 111109.
[48] A. Lakhtakia, On determining gas concentrations using dielectric thin-film helicoidal bianisotropic medium bilayers, Sens. Actuators B: Chem. 52 (1998) 243–250.
[49] T.G. Mackay, A. Lakhtakia, Empirical model of optical sensing via spectral shift of circular Bragg phenomenon, IEEE Photon. J. 2 (2010) 92–101.
[50] D.M. Mattox, The Foundations of Vacuum Coating Technology Norwich, Noyes Publications, NY, USA, 2003.
[51] I. Hodgkinson, Q.h. Wu, B. Knight, A. Lakhtakia, K. Robbie, Vacuum deposition of chiral sculptured thin films with high optical activity, Appl. Opt. 39 (2000) 642–649.
[52] M.R. Hoffmann, S.T. Martin, Y. Choi, D.W. Bahnemann, Environmental applications of semiconductor photocatalysis, Chem. Rev. 95 (1995) 69–96.
[53] P.D. Sunal, A. Lakhtakia, R. Messier, Simple model for dielectric thin-film helicoidal bianisotropic media, Opt. Commun. 158 (1998) 119–126.
[54] J.A. Sherwin, A. Lakhtakia, I.J. Hodgkinson, On calibration of a nominal structure–property relationship model for chiral sculptured thin films by axial transmittance measurements, Opt. Commun. 209 (2002) 369–375.
[55] Lakhtakia A (Ed.), Selected Papers on Linear Optical Composite Materials Bellingham, SPIE, WA, USA, 1996, p. xiv.
[56] K. Yokota, K. Nakamura, T. Sasakawa, T. Kamatani, Deposition of titanium oxide films with high dielectric constants on silicon by an ion beam assist deposition technique, Jpn. J. Appl. Phys. 40 (2001) 718–723.
[57] J.R. Gee, I.J. Hodgkinson, H.A. Macleod, Moisture-dependent anisotropic effects in optical coatings, Appl. Opt. 24 (1985) 3188–3192.
[58] R. Wang, N. Sakai, A. Fujishima, T. Watanabe, K. Hashimoto, Studies of surface wettability conversion on TiO single-crystal surfaces, J. Phys. Chem. B 103 (1999) 2188–2194.

[59] S.M. Pursel, M.W. Horn, Prospects for nanowire sculptured-thin-film devices, J. Vac. Sci. Technol. B 25 (2007) 2611–2615.
[60] S.M. Pursel, M.W. Horn, A. Lakhtakia, Tuning of sculptured-thin-film spectral-hole filters by postdeposition etching, Opt. Eng. 46 (2007) 04057.

Biographies

Yan Jun Liu is now a postdoctoral scholar at the Department of Engineering Science and Mechanics in the Pennsylvania State University. He received his B.Eng. in optoelectronics from Shandong University, China, in 2000, an M.S. in optics from Fudan University, China, in 2003, and a Ph.D. in photonics from Nanyang Technological University, Singapore, in 2007. He is a member of Society for Information Display (SID) since 2004. He has significant experience in optical holography, optical memories, displays, and liquid crystal photonics, and has authored/co-authored more than 20 journal publications in these fields.

Jinjie Shi received his B.S. and M.S. in microelectronics from Peking University at China in 2002 and 2005, respectively. He received his Ph.D. in Engineering Science and Mechanics from the Pennsylvania State University in 2009. His research interests are in micro/nano-electro-mechanical-system (MEMS/NEMS), micro/nano acoustics, microfluidics, sensors/actuators, and nanophotonic devices. He has published more than 20 technical papers in these fields.

Fan Zhang received his Ph.D. in the Department of Engineering Science and Mechanics at the Pennsylvania State University in 2009. His research interests are in semiconductor optoelectronic devices and circuits, bioelectronic and biophotonic devices, micro-opto-electro-mechanical systems (MOEMS). Currently, he works as a Research Engineer for Cree Corporation.

Huinan Liang received his Ph.D. in Engineering Science and Mechanics from the Pennsylvania State University in 2008. Currently, he is a Process Engineer at Intel Corporation. His research interests include semiconductor devices and micro/nano-electro-mechanical-system (MEMS/NEMS).

Jian Xu received B.S. (1992), M.S. (1998), and Ph.D. (2003) degrees from Tianjin University, the University of Virginia, and the University of Michigan, respectively. He is an associate professor in the Department of Engineering Science and Mechanics at the Pennsylvania State University. His research interests include micro-opto-electro-mechanical system (MOEMS), nonlinear optics, and quantum dots.

Akhlesh Lakhtakia obtained a B.Tech. in Electronics Engineering from the Institute of Technology, Banaras Hindu University, India in 1979; M.S. and Ph.D. in Electrical Engineering from the University of Utah, USA in 1981 and 1983, respectively; and D.Sc. in Electronics Engineering in 2006 from Banaras Hindu University. Currently, he is the *Charles Godfrey Binder* (*Endowed*) *Professor* of Engineering Science and Mechanics at the Pennsylvania State University. He has published more than 675 journal articles. He became the first Editor-in-Chief of SPIE's online *Journal of Nanophotonics*. His current research interests lie in the electromagnetics of complex materials, sculptured thin films, carbon nanotubes, nanoengineered metamaterials, biomimetics, and negative refraction.

Stephen J. Fonash holds the Bayard D. Kunkle Chair Professor in Engineering Sciences at the Pennsylvania State University. His activities at Penn State include serving as the director of Penn State's Center for Nanotechnology Education and Utilization (CNEU), director of the National Science Foundation Advanced Technology Education Center, and director of the Pennsylvania Nanofabrication Manufacturing Technology Partnership. He is a fellow of the Institute of Electrical and Electronics Engineers and a fellow of the Electrochemical Society. His research activities encompass the processing and device physics of micro- and nanostructures including solar cells, sensors, and transistors. He has published over 300 refereed papers in these areas.

Tony Jun Huang received a Ph.D. in Mechanical and Aerospace Engineering from the University of California, Los Angeles (UCLA) in 2005, and B.S. and M.S. in Energy and Power Engineering from Xi'an Jiaotong University, Xi'an, China, in 1996 and 1999, respectively. He is an associate professor in the Department of Engineering Science and Mechanics at the Pennsylvania State University. His research interests include biomedical nanoelectromechanical systems (BioNEMS), molecular mechanics, nanomaterials/nanodevices, and micro fluidics.